J. Fluid Mech. (1966), *vol.* 24, *part* 1, *pp.* 99–112
Printed in Great Britain

Inviscid hypersonic flow on cusped concave surfaces

By PHILIP A. SULLIVAN†
Imperial College, London

(Received 7 June 1965)

An analysis of the exact equations of the inviscid flow of a perfect gas over cusped concave bodies is described. The field is examined in the limit of infinite free-stream Mach number M_∞. The slope of the shock wave in a small region adjacent to the leading edge is strongly dependent on M_∞, while much further downstream the shock-wave slope is controlled primarily by the body slope. Consequently the region near the leading edge introduces into the field downstream a thin layer of gas, adjacent to the body, where the entropy is much lower than that of the gas above it. This layer is so dense that the gas velocity along it is not appreciably slowed by the pressure gradient along the body. However, it is so thin that there is little pressure change across it.

The well-known self-similar solutions to the hypersonic small-disturbance equations have previously only been used to study the flow on blunted slender convex surfaces. They are known to behave singularly at the body. It is shown that there is a region on concave power-law shapes where the self-similar solutions are the correct first approximation to the exact inviscid equations in the limit $M_\infty \to \infty$; and that, further, they predict the correct first-order surface pressure.

Numerical results for surface pressure from the similar solutions are presented, and comparisons are made with certain approximate theories available for more general shapes. Pressure measurements taken on a cubic surface in the Imperial College gun tunnel are presented and compared with the theoretical distributions.

1. Introduction

In the development of the theory of inviscid hypersonic flow, applications have been primarily confined to convex bodies. Recently, however, interest in such problems as the separated boundary layer and the hypersonic intake has directed attention towards the corresponding concave-surface problem.

Inviscid concave-surface flows can differ considerably from those over a convex surface. Typically, leading-edge bluntness effects tend to be much less important. The compression waves on a concave surface can form shock waves in addition to the shock wave generated by the leading edge. Shear layers and strong finite reflected Mach waves are generated by this shock formation, and by the interaction of this shock wave with the leading-edge shockwave. Such flow fields generally have a complicated structure. For simplicity this paper is limited to the discussion of the flow fields in which there is only one concave shock wave present.

† Now at Institute for Aerospace Studies, University of Toronto, Toronto, Canada.

Hypersonic small-disturbance theory introduces two major simplifications into the analysis. One is the well-known hypersonic similarity rule. The other is the equivalence principle, by which a steady hypersonic slender-body flow can be reduced to an unsteady flow in a space of one fewer dimensions.

The equivalence principle allows the well-known self-similar solutions to the equations of one-dimensional unsteady flow to be applied to the two-dimensional steady hypersonic flow. The most comprehensive available treatment of these solutions is given by Sedov (1959, pp. 136–304), and a discussion of their application to hypersonic flow is given by Hayes & Probstein (1959, ch. 2). There are several conditions for the existence of self-similarity. The gas must be both thermally and calorically perfect. The body shape in the equivalent hypersonic flow must be plane or axially symmetric, and have the form $y_b = Dx^k$, where x is the streamwise variable, and y is the lateral variable. The free-stream Mach number M_∞ must be such that the shock-wave angle is very much larger than that of a free-stream Mach wave: $\sigma \gg 1/M_\infty$. The oblique shock relations can then be taken as those for $M_\infty = \infty$, and the shock is said to be strong. The limiting shock shape is then similar to the body shape: $y_s = D_s x^k$. The similar solution can be regarded as a first approximation to the asymptotic development of the field in powers of $\delta = M_\infty^{-2}$.

When the exponent $k < 1$, the solution represents the flow in the slender regions of a blunted slender convex surface. With $k = 1$ the body is a wedge or cone. When $k > 1$ the body is cusped and concave. Only those solutions for $k \leqslant 1$ have been discussed in any detail in the literature.

There are a number of physical difficulties associated with the similar solutions. When $k < 1$ the equivalence principle fails near the leading edge, since the body slope $dy_b/dx \to \infty$ as $x \to 0$; and when $k > 1$ it fails far downstream since $dy_b/dx \to \infty$ as $x \to \infty$. The strong-shock assumption fails far downstream from the leading edge when $k < 1$, since $dy_b/dx \to 0$ as $x \to \infty$; and it fails for a small region near the origin when $k > 1$, since $dy_b/dx \to 0$ as $x \to 0$. The similar solutions behave singularly near the body. When $k < 1$ the expression for the temperature becomes infinite as $y \to y_b$, and when $k > 1$ the expression for the density becomes infinite as $y \to y_b$. In both cases the pressure remains finite. This behaviour was pointed out by Lees & Kubota (1957). The systematic investigation of the regions where the similar solutions behave unsatisfactorily in the hypersonic flow was not undertaken until quite recently. Yakura (1962), by considering the inverse problem, and Freeman (1962), by considering the direct problem, have given more satisfactory interpretations of the behaviour of the field in these regions for $k < 1$.

In this paper the behaviour of the field on a cusped concave body in the limit $M_\infty \to \infty$ is examined. The structure of the field adjacent to the origin, where the shock is never strong, is discussed; and its effect on the field downstream is examined. An analysis of the field near the body, where on power-law surfaces the self-similar solutions behave singularly, is given. It is shown that there is a region on power-law surfaces where the similar solutions are the correct first approximation to the exact inviscid equations in the limit $M_\infty \to \infty$.

Some values of surface pressure obtained from the similar solutions for two-

dimensional surfaces are presented and are compared with values calculated by certain approximate methods which are available for more general shapes.

Finally, to demonstrate the usefulness of the inviscid concept of hypersonic flow on concave surfaces, some pressure measurements obtained on a cubic surface in the Imperial College hypersonic gun tunnel will be described.

2. Singular behaviour of the similar solutions

Consider the inviscid hypersonic flow of a gas about a body in which there is only one shock wave present. The well-known oblique shock relations can be put in the form:

$$\left.\begin{aligned} p_s/\rho_\infty U^2 &= (\delta/\gamma)+\{2/(\gamma+1)\}\{\sin^2\sigma-\delta\}, && (a)\\ \rho_\infty/\rho_s &= \{(\gamma-1)/(\gamma+1)\}+\{2/(\gamma+1)\}\{\delta/\sin^2\sigma\}, && (b)\\ v_s/U &= \{2/(\gamma+1)\}\cot\sigma\{\sin^2\sigma-\delta\}, && (c)\\ (u_s/U)-1 &= -\{2/(\gamma+1)\}\{\sin^2\sigma-\delta\}, && (d) \end{aligned}\right\} \tag{2.1}$$

where the shock shape is given by $y = y_s(x)$; $\tan\sigma = dy_s/dx$. The quantity p is the pressure, ρ is the density, u is the velocity in the x-direction, v is the velocity in the y-direction, and γ is the ratio of the specific heats. U is the free-stream velocity, and ρ_∞ is the free-stream density. The subscript s denotes conditions immediately downstream of the shock wave.

In a hypersonic flow about a slender body with a characteristic slope τ, σ is at most $O(\tau)$ for sufficiently large M_∞. Then inspection of the oblique-shock relations shows that

$$p_s/\rho_\infty U^2 \sim O(\tau^2), \quad \rho_s/\rho_\infty \sim O(1), \quad v_s/U \sim O(\tau), \quad u_s/U = 1+O(\tau^2).$$

The hypersonic small-disturbance equations are then derived from the exact inviscid equations by the usual argument. They are

$$\left.\begin{aligned} U\frac{\partial\rho}{\partial x}+\frac{\partial}{\partial y}(\rho v)+j\rho v/y &= 0, && (a)\\ U\frac{\partial v}{\partial x}+v\frac{\partial v}{\partial y}+\frac{1}{\rho}\frac{\partial p}{\partial y} &= 0, && (b)\\ U\frac{\partial}{\partial x}(p/\rho^\gamma)+v\frac{\partial}{\partial y}(p/\rho^\gamma) &= 0, && (c) \end{aligned}\right\} \tag{2.2}$$

together with an equation for $(u - U)$ which is of higher order, and is not required here. The small disturbance approximations to the shock relations are equations (2.1) with $\sin\sigma \simeq \sigma \simeq \tan\sigma$. The small-disturbance approximation to the body condition $v/u = dy_b/dx$ is

$$v_b = U\,dy_b/dx \tag{2.3}$$

at $y = y_b(x)$; the subscript b denotes conditions at the body.

By an elegant application of dimensional methods, Sedov (1959, p. 146) shows that with p, ρ and v replaced by

$$P = \frac{p}{\rho_\infty U^2}\frac{x^2}{y^2}, \quad R = \frac{\rho}{\rho_\infty}, \quad V = \frac{v}{U}\frac{x}{y}, \tag{2.4}$$

and the independent variables replaced by

$$\lambda = y/Dx^k, \quad y_b = Dx^k, \tag{2.5}$$

then equations (2.2*a*) to (2.2*c*) for a power-law body reduce to ordinary differential equations. If it is further assumed that $\sigma \gg 1/M_\infty$, then the shock shape approaches the form $y_s = D_s x^k$. The oblique shock relations for p, ρ and v then become

$$P_s = \{2/(\gamma+1)\}\, k^2, \quad R_s = (\gamma+1)/(\gamma-1), \quad V_s = 2k/(\gamma+1), \tag{2.6}$$

at $\lambda_s = D_s/D$. The body condition (equation (2.3)) becomes $V_b = k$ at $\lambda = 1$.

It is more convenient to use the quantity $\xi = V - k$ as the independent variable. The shock wave then corresponds to the point $\xi = -\{(\gamma-1)/(\gamma+1)\}k$, and the body to the point $\xi = 0$. If the quantity $Z = \gamma P/R$ is introduced, the problem can be reduced to one differential equation in Z and two quadratures. Z is proportional to the temperature. The equation for Z is

$$\frac{dZ}{d\xi} = \frac{\begin{array}{r} Z\,[\{2+j(\gamma-1)\}\xi^3 + \{(k-1)(3-\gamma)+j(\gamma-1)k\}\xi^2 \\ +k(k-1)(1-\gamma)\xi - 2Z(\xi+(k-1)/\gamma)] \end{array}}{\xi[\xi^3+(2k-1)\xi^2+k(k-1)\xi - Z\{(1+j)\xi+2(k-1)/\gamma+(j+1)k\}]}. \tag{2.7}$$

The equations for λ and R are not required here. Equation (2.7) is a variant of the form given for Z by Sedov (1959, p. 155).

Consider now the behaviour of equation (2.7) near the body, that is, as $\xi \to 0$. It can be easily shown that the only self-consistent assumption is that $Z/\xi \to \infty$ as $\xi \to 0$, whence it follows that

$$Z \simeq Z_0 \xi^\alpha, \tag{2.8}$$

where

$$\alpha = \frac{2(k-1)}{2(k-1)+\gamma k(1+j)} \tag{2.9}$$

and Z_0 is a constant. When $k < 1$, $Z \to \infty$ as $\xi \to 0$, but when $k > 1$, $Z \to 0$ as $\xi \to 0$. A similar analysis shows that $R \simeq R_0 \xi^{-\alpha}$, $\lambda = 1+\lambda_1\xi$, $P = P_b + P_1\xi$, where R_0, λ_1, and P_1 are constants. Thus in the similar solutions the density and the temperature show a singular behaviour near the body, but the pressure remains finite. When $k < 1$, $Z \to \infty$ and $R \to 0$ as $\lambda \to 1$, whereas, when $k > 1$, $Z \to 0$ and $R \to \infty$ as $\lambda \to 1$.

3. The leading-edge region

To interpret the behaviour of the similar solutions near the body for $k > 1$, it is necessary to study the behaviour of the field near the leading edge in the limit $M_\infty \to \infty$ or $\delta \to 0$, and to consider the leading-edge effect on the field downstream of it. Although the similar solutions are the major interest, the remarks to be made in this and the following section apply to any cusped concave body, and can easily be generalized to include any concave surface which has a leading-edge angle θ_L such that $\theta_L = O(1/M_\infty) = O(\delta^{\frac{1}{2}})$.

The formation of a shock wave by a cusped surface is discussed by Courant & Freidrichs (1948, pp. 107–15 and p. 294). For the present purpose it is sufficient to note that the Mach waves generated by the cusped surface always intersect

at a sufficient distance from the surface, and that the envelope of the region where the Mach waves intersect forms a cusp. This cusp is the nearest point of the envelope to the leading edge of the surface. Because the solution inside the envelope is unacceptable, it is assumed in the classical treatment that a shock wave grows from the envelope cusp. It is here assumed that this shock wave is the only one present in the inviscid hypersonic flow on a cusped surface. If the curvature of the cusped surface at the leading edge is zero, then the envelope cusp lies on the Mach wave which passes through the leading edge; if it is not zero, the envelope cusp lies between the leading-edge Mach wave and the surface. In both cases the envelope cusp must lie upstream of the point Q, defined as the intersection of the extrapolation of the leading-edge Mach wave and the surface. In the latter case the shock wave must cross into the free stream upstream of Q.

The shape of the cusped surface may be expressed in the form

$$y_b = Dx^k + O(x^{k+1}) \quad \text{as} \quad x \to 0,$$

where $k > 1$. The equation of the Mach wave starting from the leading edge is $y = x\tan(1/M_\infty)$; and as $M_\infty \to \infty$ this becomes $y = x\delta^{\frac{1}{2}}$. Thus $x_Q = [\delta^{\frac{1}{2}}/D]^{1/k-1}$, $y_Q = D[\delta^{\frac{1}{2}}/D]^{k/k-1}$ and $(dy_b/dx)_Q = k\delta^{\frac{1}{2}}$. This suggests that near Q, and for some region downstream of Q, the shock slope $\sigma \sim O(\delta^{\frac{1}{2}})$. That part of the field on a cusped body for which $\sigma \sim O(\delta^{\frac{1}{2}})$ is called the leading-edge region. It is to be distinguished from the very much smaller region extending downstream from the leading edge where the classical small-perturbation approximation

$$\sigma \simeq \delta^{\frac{1}{2}} = 1/M_\infty$$

holds.

The orders of magnitude of the quantities in the leading-edge region may be estimated by using the oblique-shock relations for that portion of the shock wave in the leading-edge region and in the free stream. Thus, with

$$\sin\sigma \simeq \tan\sigma \simeq O(\delta^{\frac{1}{2}})$$

in equations (2.1), we have

$$\left.\begin{aligned} p/\rho_\infty U^2 &\sim O(\delta), & \rho/\rho_\infty &\sim O(1), \\ v/U &\sim O(\delta^{\frac{1}{2}}), & u/U &\sim 1 + O(\delta), \\ x/l &\sim O(\delta^{1/2(k-1)}), & y/l &\sim O(\delta^{k/2(k-1)}), \end{aligned}\right\} \tag{3.1}$$

where l is a typical length. A convenient length l is $D^{1/(1-k)}$. These are, of course, the relative orders of magnitude required to derive the small-disturbance equations. Thus, in the limit $\delta \to 0$, the first approximation to the exact inviscid equations in the leading-edge region is always the hypersonic small-disturbance equations. However, since $\sigma \sim O(\delta^{\frac{1}{2}})$, it is not possible to use the strong-shock approximation in the leading-edge region; even on power-law shapes it is not possible to obtain a solution except by additional approximation or numerical methods.

4. The low-entropy layer

Sufficiently far downstream of the leading edge, the slope of the shock wave depends primarily on the body slope, and in the limit is independent of M_∞; that is $\sigma \sim O(1)$ as $\delta \to 0$. Hence the limiting properties of the field immediately behind this part of the shock wave must also be independent of M_∞. However, the limiting field properties in the leading-edge region are strongly dependent on M_∞. It follows that the leading-edge region introduces into the field downstream a layer of gas, adjacent to the body, in which certain field properties are strongly dependent on M_∞. Moreover, the entropy in the leading-edge

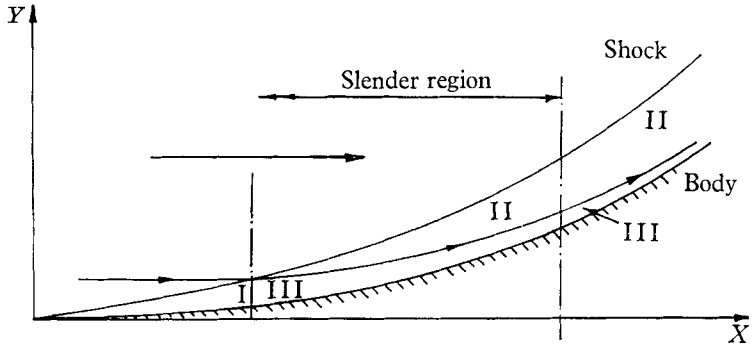

FIGURE 1. The flow regions on a cusped concave surface immersed in an inviscid hypersonic flow.

region and in the layer it introduces downstream is not much greater than the free-stream entropy. But the increase in entropy across that part of the shock wave where $\sigma \sim O(1)$ as $\delta \to 0$ is $O(\ln M_\infty^2)$ as $\delta \to 0$. For this reason, the layer adjacent to the body is called here a low-entropy layer. The regions in the field on a cusped body are depicted in figure 1. Region I is the leading-edge region. Region II—called the outer region—contains the fluid which crossed the shock wave downstream of I. Region III is the low-entropy layer; it contains the gas which passes through the region I. Since I is vanishingly small in the limit $\delta \to 0$, then III must also be vanishingly thin in that limit.

Consider the orders of magnitude of the field properties in III. From equation (3.1) $y_s \sim O(y_b) \sim O(\delta^{k/2(k-1)})$ in I, so that the mass flux through I, and hence through III, is

$$\psi_s/\rho_\infty U l^{1+j} = y_s^{1+j} \sim O(\delta^{k(1+j)/2(k-1)}), \tag{4.1}$$

where ψ denotes the stream function. We expect the pressure in III to be of the order of the pressure behind the shock in II. Thus $p/\rho_\infty U^2 \sim O(1)$ as $\delta \to 0$ in III, since $\sigma \sim O(1)$ as $\delta \to 0$ in II. But from equation (3.1) $\rho/\rho_\infty \sim O(1)$ and $p/\rho_\infty U^2 \sim O(\delta)$ in I. Since the quantity p/ρ^γ is constant between points on a streamline not cut by a shock wave, it follows that in III the density ratio ρ/ρ_∞ is $O(\delta^{-1/\gamma})$. The density distribution is thus strongly Mach-dependent and $\rho/\rho_\infty \to \infty$ as $\delta \to 0$. We shall assume that the velocity along III remains of the

order U. It then follows from equation (5.1) and the behaviour of the density in III that the thickness of III must be

$$(y-y_b)_{\mathrm{III}} \sim O(\delta^{\{k(1+j)/2(k-1)\}+1/\gamma}) = O(\delta^{1/\alpha\gamma}), \tag{4.2}$$

where α is the quantity defined in equation (2.9) for the similar solutions.

To construct the equations of the low-entropy layer, the usual boundary-layer-type co-ordinates are introduced. A point is specified by its distance n along a normal to the body surface and arc length s along the body measured from some suitable reference point. If v_n and v_s are the components of velocity in the n- and s-directions respectively, then the equations of inviscid motion of a perfect gas are

$$\frac{\partial}{\partial s}(\rho v_s y^j) + \frac{\partial}{\partial n}\{\rho v_n y^j(1+n/R)\} = 0, \tag{4.3}$$

$$\frac{Rv_s}{R+n}\frac{\partial v_s}{\partial s} + v_n\frac{\partial v_s}{\partial n} + \frac{v_s v_n}{R+n} + \frac{1}{\rho}\frac{R}{R+n}\frac{\partial p}{\partial s} = 0, \tag{4.4}$$

$$\frac{Rv_s}{R+n}\frac{\partial v_n}{\partial s} + v_n\frac{\partial v_n}{\partial n} - \frac{v_s^2}{R+n} + \frac{1}{\rho}\frac{\partial p}{\partial n} = 0, \tag{4.5}$$

$$\frac{Rv_s}{R+n}\frac{\partial}{\partial s}(p/\rho^\gamma) + v_n\frac{\partial}{\partial n}(p/\rho^\gamma) = 0, \tag{4.6}$$

where $R(x)$ is the longitudinal curvature of the body profile $y = y_b(x)$.

Now, in III, $n \sim O(\delta^{1/\alpha\gamma})$, and we have assumed $v_s/U \sim O(1)$. Inspection of the continuity equation shows that, if the analysis is to yield non-trivial results, then we must have $v_n \sim O(\delta^{1/\alpha\gamma})$. The following system of reduced variables is introduced:

$$\left.\begin{aligned} p/\rho_\infty U^2 &= p', & \rho/\rho_\infty &= \delta^{-1/\gamma}\rho', \\ v_n/U &= \delta^{1/\alpha\gamma}v_n', & v_s/U &= v_s', \\ s/l &= s', & n/l &= \delta^{1/\alpha\gamma}n', \end{aligned}\right\} \tag{4.7}$$

where the primed variables are assumed to be $O(1)$ as $\delta \to 0$ in III. The first-order approximations to equations (4.3) to (4.6) are

$$\frac{\partial}{\partial s'}(\rho' v_s' y^j) + \frac{\partial}{\partial n'}(\rho' v_n' y^j) = 0, \tag{4.8}$$

$$v_s'\frac{\partial v_s'}{\partial s'} + v_n'\frac{\partial v_s'}{\partial n'} = 0, \tag{4.9}$$

$$\partial p'/\partial n' = 0, \tag{4.10}$$

$$v_s'\frac{\partial}{\partial s'}(p'/\rho'^\gamma) + v_n'\frac{\partial}{\partial n'}(p'/\rho'^\gamma) = 0. \tag{4.11}$$

According to equation (4.9) v_s is constant along streamlines. In I, $u = U + O(\delta)$ so that, in III,

$$v_s(s', n') = v_s(s' = 0, n') = U. \tag{4.12}$$

Equation (4.10) asserts that the pressure is constant along normals to the surface. Hence in the limit $\delta \to 0$

$$p'(s', n' = 0) = p_b' = p'(s', n') = p'(s', n' = \infty) = p'(s, 0), \tag{4.13}$$

where $p'(s, 0)$ is the pressure at the inner edge of II. The streamline distribution in III is given by

$$n(\psi) = \frac{1}{y_b^j(s)\, p_b(s)\, U} \int_0^{\psi} \frac{d\psi_0}{\phi(\psi_0)},$$

where $\phi = p/\rho^{\gamma}(\psi)$ is given only by a solution for region I. However, since the surface streamline does not cross a shock wave, the surface density is given by the simple expression

$$\rho_b/\rho_\infty = \{\gamma p'(s, 0)\, M_\infty^2\}^{1/\gamma}$$

and $\rho_b/\rho_\infty \to \infty$ as $M_\infty \to \infty$.

The physical interpretation of the above analysis is as follows. In the leading-edge region the speed of the gas is not reduced much below its free-stream value. Downstream in the low-entropy layer, the density of the gas becomes so high that the momentum of the gas is large and the pressure gradient along the body cannot slow it appreciably. The gas speed remains close to the free-stream value. However, the layer is so thin that there is little pressure difference across it. Then the pressure at the body is, to the first order, the same as that at the inner edge of II.

Consider now the effect of the low-entropy layer on the solution in II. Since the thickness of III is $O(\delta^{1/\alpha\gamma})$, the first approximation to the inner-boundary condition on II is just the usual body condition

$$(v/u)_{n=0} = dy_b/dx + O(\delta^{1/\alpha\gamma}). \tag{4.14}$$

It follows from equation (2.1) that the error introduced into the solution in II by using the strong-shock approximation is $O(\delta)$. When $k > 1$,

$$1/\alpha\gamma > \{2 + (j+1)\gamma\}/2\gamma,$$

so that $1/\alpha\gamma > 1$ for the usual values of γ. Typically, for $k = 3$ and $\gamma = 1{\cdot}4$, $1/\alpha\gamma = 1{\cdot}61$ if $j = 0$, and $1/\alpha\gamma = 2{\cdot}21$ if $j = 1$. Thus, the error imposed on the solution in II by equation (4.14) is always of higher order than that imposed by using the strong-shock approximation.

The scaling of the variables in III shows that the error imposed on the first approximation to the normal-momentum equation (4.10) by neglecting the convective terms in equation (4.5) is $O(\delta^{(1/\gamma)(2/\alpha-1)})$, and by neglecting the centrifugal term is $O(\delta^{(1/\gamma)(1/\alpha-1)}) = O(\delta^{k(1+j)/2(k-1)})$. The quantity $k(1+j)/2(k-1) < 1$ only if $j = 0$ and when $k > 2$. Hence the error incurred by using equation (4.13) to estimate the surface pressure from a solution in II is of lower order than that imposed by the strong-shock approximation on plane shapes if $k > 2$. By retaining the centrifugal term in equation (4.10) and using equation (4.12), a very simple correction for the centrifugal pressure rise across III can be given, provided that a solution for region I is available. The surface pressure at the body is given by

$$p(n' = 0) = p_b = p(n = 0) + U\psi_1/R,$$

where $\psi_1 \sim O(\delta^{k/2(k-1)})$ is the mass flux of gas through I.

The characteristic feature of region II is that in the limit $M_\infty \to \infty$ or $\delta \to 0$ the strong shock approximation can be applied to the shock-wave relations. But even with this simplification it is not generally possible to obtain a solution in region II in closed form without making additional approximations.

The analysis of the low-entropy layer has been made without using the slender-body approximation. However, in the limit $M_\infty \to \infty$ there must be a region on a cusped surface where the body is slender and hence $\sigma \ll 1$, but where $\sigma/M_\infty \gg 1$. Both the hypersonic small-disturbance equations and the strong-shock approximation can be applied in this region. In fact, immediately downstream of I there must be a region where $\sigma \to 0$ as $\delta \to 0$ but where $\sigma/\delta^{\frac{1}{2}} \to \infty$ as $\delta \to 0$. This may be expressed as $\sigma \sim O(\delta^\beta)$ with $\frac{1}{2} > \beta > 0$. Given this order assumption it is then possible to derive both the hypersonic small-disturbance equations and the strong-shock limit as the first approximation to the exact inviscid equations and the oblique-shock relations. Furthermore, by using the assumption $\sigma \sim O(\delta^\beta)$, the arguments leading to the derivation of the low-entropy-layer equations can be repeated for the slender region. Typically, ρ/ρ_∞ is $O(\delta^{(2\beta-1)/\gamma})$ in that part of the low-entropy layer for which $\sigma \sim O(\delta^\beta)$. Also, the ratio of the error imposed on the solution in II by the low-entropy layer to the error imposed by finite M_∞ at the shock wave tends to zero as $M_\infty \to \infty$, as it does far downstream. On power-law shapes, the similar solutions are the correct first approximation to the exact inviscid equations of the field in that part of II which is in the slender region.

It is instructive to compare the properties of the low-entropy layer with those of the entropy layer generated on a blunted slender body. The former is associated with the failure of the strong-shock approximation, whereas the latter is generated by the failure of the slender-body approximation at the nose. Both have constant pressure across the layer but in other respects they differ. The low-entropy layer is cold and dense, and the velocity is nearly constant across it; the entropy layer is hot and at low density, and the velocity varies rapidly across it. The entropy layer can displace the outer region by an amount which imposes a lower-order error than that imposed by the strong-shock approximation. Freeman (1962), in an analysis of the similar solutions, has shown that the thickness of the entropy layer is (in the present notation) $O(\delta^{-1/\alpha\gamma})$ where $\alpha < 0$, since $k < 1$. For $k < 2(\gamma+1)/\{2+\gamma(3+j)\}$, $(-1/\alpha\gamma) < 1$.

5. Numerical results from the similar solutions: comparison with approximate theories

The equations for the self-similar solutions were integrated for $j = 0$ and $k > 1$ on the University of London Digital Computer. Details of the method used and the tabulated numerical values are given by Sullivan (1963).

Some values of surface pressure obtained from the similar solutions are presented here, and are compared with values estimated by using certain approximate methods available for more general shapes. The approximate methods used are: (1) the simple wave (or shock expansion) theory; (2) the tangent wedge rule; (3) Newtonian plus centrifugal formula. These methods are described in the standard texts on hypersonic flow. See, for example, Hayes & Probstein (1959) and Chernyi (1961). They are used here in their small-disturbance form.

In figure 2, the quantity $P_b/k^2 = P_b/\rho_\infty U^2\theta_b^2$, obtained from the similar solutions, is plotted as a function of k for $\gamma = 1{\cdot}4$. In figure 3, P_b/k^2 is plotted as a function of γ for $k = 4$. In both cases the other estimates of P_b/k^2 are obtained

from the Newtonian plus centrifugal formula and the tangent-wedge rule for $M_\infty = \infty$. The simple-wave theory cannot be applied at $M_\infty = \infty$. According to this theory, the pressure on a cusped surface will be generated by an isentropic simple-wave compression from the free-stream static pressure. Hence (see Chernyi 1961, p. 41), when $\theta_b \ll 1$, $p_b/\rho_\infty U^2\theta_b^2 \sim \frac{1}{2}(\gamma-1)(M_\infty\theta_b)^{2/(\gamma-1)}$, where θ_b remains finite as $M_\infty \to \infty$.

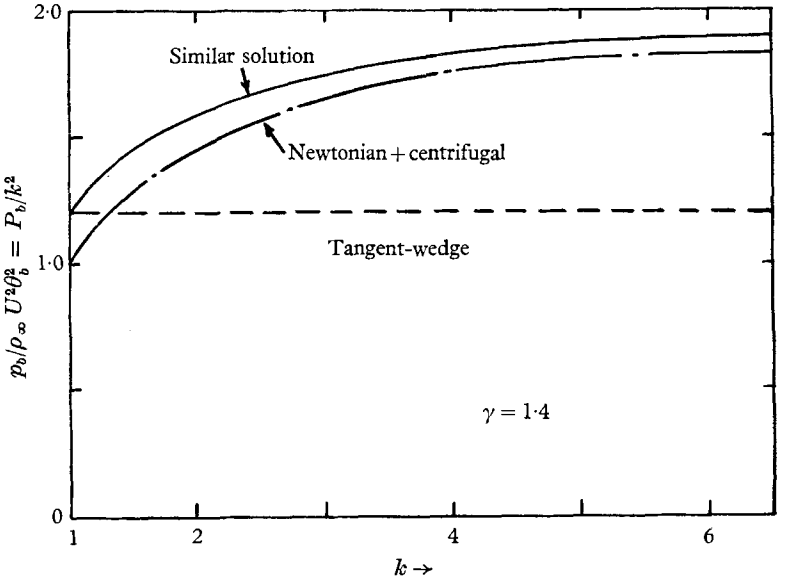

FIGURE 2. Effect of k on the non-dimensional pressure $P_b/k^2 = p_b/\rho_\infty U^2\theta_b^2$.

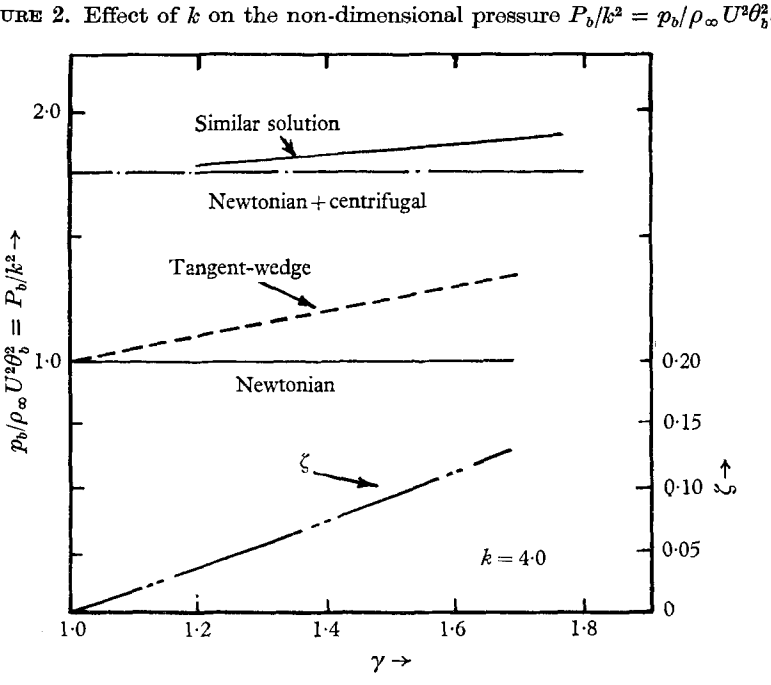

FIGURE 3. Effect of γ on the non-dimensional pressure P_b/k^2 and the shock-layer thickness $\zeta = (y_s - y_b)/y_b$.

The pressure distributions estimated for a surface having the shape $y_b = x^3/150$ are given in figure 4. In this case estimates from the simple-wave theory for $M_\infty = 7{\cdot}5$ and 10 are included to demonstrate its behaviour.

The Newtonian plus centrifugal theory agrees moderately well with the similar solutions when $\gamma = 1{\cdot}4$, and the results in figure 3 show that the agreement improves rapidly as γ approaches one. Since the tangent-wedge rule accounts only for the shock-pressure rise, the difference between the tangent-wedge estimate and that of the similar solutions is a measure of the centrifugal-pressure rise across the layer.

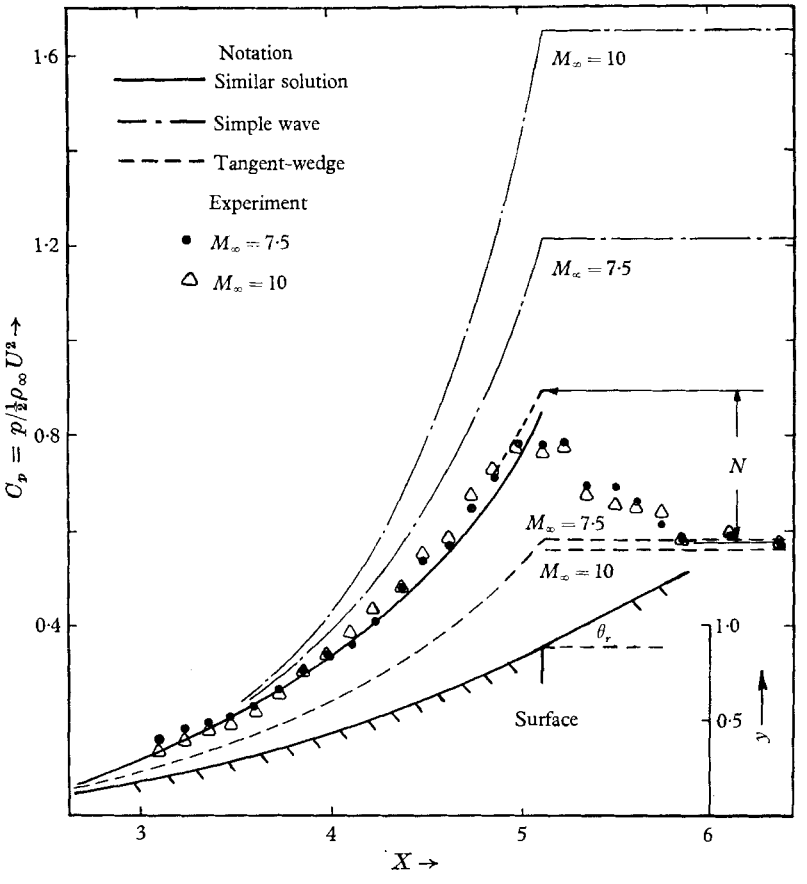

FIGURE 4. Pressure distributions on a cubic surface according to the various theories, and comparison with experiment.

The simple-wave theory overestimates the surface pressure, and the error rapidly increases as $M_\infty \rightarrow \infty$. To justify use of this theory it must be shown that the Mach waves generated at the surface (called principal waves) are much stronger than the Mach waves generated at the shock wave and streamlines and which travel toward the surface (called reflected waves). The behaviour of the simple-wave theory shown in figure 4 suggests that there are strong reflected waves present in the field. A possible explanation of this behaviour is as follows.

Part of the argument usually given to show that the reflected Mach waves generated in the flow over a slender convex surface can be very weak is that the reflected Mach waves generated at the shock tend to cancel those generated at the streamlines. Hayes & Probstein (1959, p. 268), show that the waves generated at the shock are usually compressions, and those at the streamlines are expansions. But, if their argument is repeated for a concave surface when the shock wave is also concave, it can be shown that both types of reflected wave are expansions, and must therefore add. The reflected waves should therefore be much stronger in a concave-surface flow.

In the similar solutions the shock shape is given by $y_s = \lambda_s D x^k$. Therefore, the quantity $\zeta = \lambda_s - 1$ can be used as a measure of the shock-layer thickness. In figure 3, ζ is plotted as a function of γ for $k = 4{\cdot}0$. The shock layer is fairly thin for moderate values of γ and becomes very thin as γ approaches one.

6. Experimental verification

Pressure measurements were taken on a surface having the shape described in figure 4 in the Imperial College hypersonic gun tunnel. This facility is described by Needham (1963).

The tests were conducted at nominal free-stream Mach numbers (M_∞) of 7·5 and 10. The stagnation pressure was 1590 psia and the stagnation temperature was 800 °K for all tests. With these conditions the free-stream unit Reynolds number was $6{\cdot}0 \times 10^5$/in. at $M_\infty = 7{\cdot}5$ and $3{\cdot}2 \times 10^5$/in. at $M_\infty = 10$. In the present tests, the tunnel was fitted with a conical nozzle having an exit-plane diameter of 8 in. and an included angle of 20°. Because of instrumentation limitations, measurements were only taken downstream of the point for which $\theta_b = 10°$. This point is marked by an arrow in figure 5 (plate 1). Details of the preliminary experiments, and the procedures used to correct for the ambient flow non-uniformities generated by the conical nozzle, are given by Sullivan (1963).

Figure 5 (plate 1) is a schlieren photograph of the field generated on the surface at $M_\infty = 10$. A shock wave grows from the leading edge of the model. Downstream the compression waves generate a concave shock wave which intersects the leading-edge shock wave. The concave shock wave is not visibly deflected by the leading-edge shock wave, and it follows that it is much stronger than the leading-edge shock wave at their line of intersection. The presence of the leading-edge shock wave is neglected in the interpretation of the present results. A schlieren photograph of the field taken when $M_\infty = 7{\cdot}5$ showed a similar structure.

To obtain an independent check of the centrifugal-pressure rise, the surface was extended as a ramp, that is, at constant slope $\theta_r = 28°$. The pressure at the beginning of the ramp should be that given by the similar solutions, while sufficiently far downstream the pressure should approach that generated by a wedge having the same slope as the ramp. This is the value predicted by the tangent-wedge theory. Thus, the pressure fall-off, Δp, along the ramp should approach

$$\Delta p \simeq \rho_\infty U^2 \theta_r^2 \{P_b/k^2(k,\gamma) - \tfrac{1}{2}(\gamma+1)\} \quad \text{as} \quad M_\infty \to \infty. \tag{6.1}$$

The pressure distributions obtained on the surface are given in figure 4. There is good agreement with the values predicted by the similar solutions. The pressure distribution on the ramp appears to flatten out at the end of the ramp, suggesting that the tangent-wedge value has been attained. The experimental and theoretical values of the quantity $N = \Delta p/\rho_\infty U^2\theta_r^2$ are compared in table 1. There is good agreement, but the measurements need to be confirmed by extending the ramp.

		Experimental	
	Theoretical	$M_\infty = 7{\cdot}5$	$M_\infty = 10$
N	0·55	0·54	0·58

TABLE 1

In this experiment, the photograph in figure 5 suggests that the self-similar flow was obtained only in a relatively small region at the rear of the surface. A larger region would be obtained on a surface for which $k < 3$.

7. Conclusions

Two main points emerge from the analysis. The first is that the low-entropy layer only affects the solution in the outer region by an amount which is of higher order than the Mach-number effect at the shock wave. Hence, to extend the similar solutions towards the leading edge it is initially only necessary to include Mach-number effects at the shock wave.

The second point is the usefulness of the thin-shock-layer theory for concave-surface flows. The similar solutions show that the shock layer can be very thin. This occurs partly because the centrifugal effects tend further to compress the gas in the layer. This contrasts with the behaviour on convex surfaces, where the centrifugal effects tend to throw the shock wave out from the body. Of course the thin-shock-layer theory cannot be used downstream of a discontinuity in profile slope or curvature.

Although the experiment described here gave very good agreement with the similar solutions, it would be desirable to extend the measurements toward the leading edge. It would also be of considerable interest to probe the low-entropy layer by measuring the density distribution across the shock layer.

The author acknowledges the considerable help and advice given him by Mr J. L. Stollery and Dr N. C. Freeman, both of Imperial College. The work described in this paper formed part of a Ph.D. thesis submitted to the University of London.

REFERENCES

CHERNYI, G. G. 1961 *Introduction to Hypersonic Flow.* New York: Academic Press.

COURANT, R. & FRIEDRICHS, K. O. 1948 *Supersonic Flow and Shock Waves.* New York: Interscience.

FREEMAN, N. C. 1962 An approach to second order solutions of hypersonic small disturbance theory. *NPL Aero. Rep.* no. 1035, ARC 23999.

HAYES, W. D. & PROBSTEIN, R. F. 1959 *Hypersonic Flow Theory.* New York: Academic Press.

LEES, L. & KUBOTA, T. 1957 Inviscid hypersonic flow over blunt-nosed slender bodies. *J. Aero. Sci.* **24**, 195–202.

NEEDHAM, D. A. 1963 A progress report on the Imperial College gun tunnel. *Imperial College Aero. TN* no. 118.

SEDOV, L. I. 1959 *Similarity and Dimensional Methods in Mechanics.* Moscow: Goste khizdat. English Translation (ed. M. Holt). New York and London: Academic Press.

SULLIVAN, P. A. 1963 An investigation of hypersonic flow over concave surfaces and corners. University of London, Ph.D. Thesis.

YAKURA, J. K. 1962 Theory of entropy layers and nose bluntness in hypersonic flow. *Progress in Astronautics and Rocketry*, vol. 7, *Hypersonic Flow Research.* New York: Academic Press.

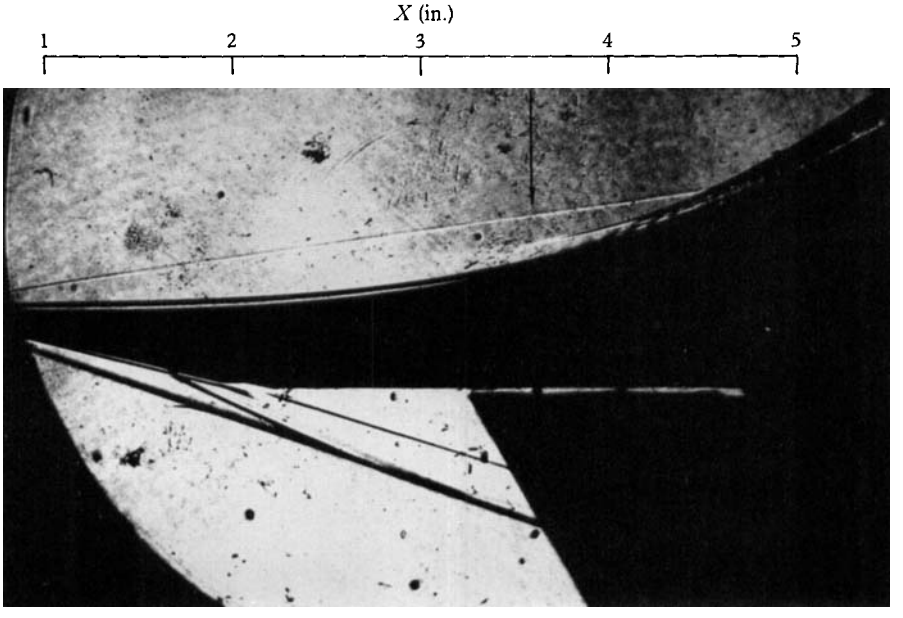

FIGURE 5. Schlieren photograph of flow generated on a cubic surface in the Imperial College hypersonic gun tunnel. $M_\infty = 10$.